

## **New Exciplex Systems Composing of Triazatruxene Donors and N-Heteroarene-Cored Acceptors**

Yuan-Cheng Hu,<sup>a</sup> Zong-Liang Lin,<sup>a</sup> Tzu-Chien Huang,<sup>b</sup> Jih-Wei Lee,<sup>b</sup> Wei-Chih Wei,<sup>a</sup> Tzu-Yu Ko,<sup>a</sup> Chun-Yuan Lo,<sup>a</sup>, Deng-Gao Chen,<sup>a</sup> Pi-Tai Chou,<sup>a</sup>, Wen-Yi Hung<sup>\*b</sup> and Ken-Tsung Wong<sup>\*a, c</sup>

<sup>a</sup>Department of Chemistry, National Taiwan University, Taipei, 10617, Taiwan.

E-mail: kenwong@ntu.edu.tw

<sup>b</sup> Department of Optoelectronics and Materials Technology, National Taiwan Ocean University, Keelung 202, Taiwan

E-mail: wenhung@mail.ntou.edu.tw

<sup>c</sup> Institute of Atomic and Molecular Science, Academia Sinica, Taipei, 10617 Taiwan

	<b>Contents</b>	<b>Page</b>
	<b>Experimental section</b>	<b>S3</b>
<b>Figure S1</b>	Cyclic voltammograms of triazatruxenes <b>Tr-Me</b> , <b>Tr-Ph</b> , <b>Tr-Tol</b> , and acceptors <b>3P-T2T</b> , <b>3P-T2P</b> and <b>3P-Pyr</b> .	<b>S9</b>
<b>Figure S2</b>	HOMO energy levels of (a) <b>Tr-Me</b> , (b) <b>Tr-Ph</b> and (c) <b>Tr-Tol</b> determined by using photoelectron yield spectroscopy (Riken AC-2)	<b>S9</b>
<b>Figure S3</b>	UV-Vis and emission spectra of (a) donors ( <b>Tr-Me</b> , <b>Tr-Ph</b> and <b>Tr-Tol</b> ) and (b) acceptors ( <b>3P-T2T</b> , <b>3P-T2P</b> and <b>3P-Pyr</b> ) in neat film recorded at room temperature.	<b>S10</b>
<b>Figure S4</b>	UV-Vis of D-A blend film and their corresponding composing materials recorded in room temperature.	<b>S11</b>
<b>Figure S5</b>	Transient PL decays of donor: acceptor (1:1) film at room temperature.	<b>S12</b>
<b>Figure S6</b>	Time-resolved PL spectra of the donor: acceptor (1:1) films at 300 K. Prompt (black line: delay = 0 ns, gate width 100 ns) and delayed 1 $\mu$ s (red line: gate width = 10 $\mu$ s) components of the PL spectra. $\Delta E_{ST}$ is calculated from the energy difference between the emission onsets of prompt and delayed signals.	<b>S12</b>
<b>Figure S7</b>	Typical transient photocurrent signals for hole (a) <b>Tr-Ph</b> ( $E = 3.78 \times 10^5$ V/cm) and (c) <b>Tr-Tol</b> ( $E = 8.17 \times 10^5$ V/cm). Insets are the double logarithmic plots of (a)/(c). Electron and hole mobilities versus $E^{1/2}$ for (b) <b>Tr-Ph</b> and (d) <b>Tr-Tol</b> .	<b>S13</b>
<b>Figure S8</b>	(a) UV-Vis and emission spectra and (b) cyclic voltammogram of <b>(DT)<sub>2</sub>Bth2CN</b> .	<b>S14</b>
<b>Figure S9</b>	(a) J-V-L characteristics, (b) EQE and PE as a function of luminance and (c) EL spectra of <b>Tr-Tol:3P-T2P</b> hosted devices with various doping concentrations.	<b>S14</b>
<b>Table S1</b>	Characterization of <b>(DT)<sub>2</sub>Bth2CN</b>	<b>S15</b>
<b>Table S2</b>	The PLQY and TRPL characteristics of the 10 wt% <b>(DT)<sub>2</sub>Bth2CN</b> doped in D:A blended films	<b>S15</b>
<b>Figure S10</b>	The <sup>1</sup> H NMR of <b>Tr-Tol</b>	<b>S16</b>
<b>Figure S11</b>	The <sup>13</sup> C NMR of <b>Tr-Tol</b>	<b>S16</b>
<b>Figure S12</b>	The <sup>1</sup> H NMR of <b>3P-T2P</b>	<b>S17</b>
<b>Figure S13</b>	The <sup>13</sup> C NMR of <b>3P-T2P</b>	<b>S17</b>
<b>Figure S14</b>	The <sup>1</sup> H NMR of <b>3P-Pyr</b>	<b>S18</b>
<b>Figure S15</b>	The <sup>13</sup> C NMR of <b>3P-Pyr</b>	<b>S18</b>
<b>Figure S16</b>	The <sup>1</sup> H NMR of <b>(DT)<sub>2</sub>BTh2CN</b>	<b>S19</b>
<b>Figure S17</b>	The <sup>13</sup> C NMR of <b>(DT)<sub>2</sub>BTh2CN</b>	<b>S19</b>

## Experimental Section

### Materials

10,15-dihydro-5H-diindolo[3,2-a:3',2'-c]carbazole<sup>[1]</sup>, 1,3-dibromobenzo[c]thiophene-5,6-dicarbonitrile<sup>[2]</sup>, 2,4,6-tris(3-bromophenyl)pyrimidine<sup>[3]</sup>, 2,4,6-tris(3-bromophenyl)pyridine<sup>[4]</sup>, **Tr-Me**<sup>[5]</sup>, **Tr-Ph**<sup>[6]</sup> and **3P-T2T**<sup>[7]</sup> were prepared according to reported literatures. All the chemicals and reagents were used without purification from commercial sources unless otherwise noted. Solvents for analysis and reaction were purified by distillation with drying equipment before use.

### Material characterization

Thermogravimetric analysis (TGA) and differential scanning calorimetry (DSC) were conducted under a nitrogen atmosphere at a heating rate of 10 °C/min on a platinum pan via a TA Instruments Q500 TGA (V20.13 Build 39) and Netzsch 204 F1. NMR spectra were measured in CDCl<sub>3</sub> or CD<sub>2</sub>Cl<sub>2</sub> using Varian (Utility 400) spectrometer for <sup>1</sup>H NMR (400 MHz) and <sup>13</sup>C NMR (100 MHz). Optical absorption measurements were conducted by a JASCO V-670 spectrophotometer. TRPL lifetime studies were performed with an Edinburgh FL 900 photon-counting system using a hydrogen-filled lamp as the excitation source. The emission decays were fitted by the sum of exponential functions with a temporal resolution of ~300 ps via the deconvolution of instrument response function. The charging voltage of the ICCD was open at various delay times with an adjustable gated window synchronized with the firing time of the excitation pulse. In this study, the third harmonic (355 nm, fwhm ~8 ns) of an Nd:YAG laser (Continuum Surelite) was used as the excitation pulse. For the PL spectrum measurement, the thin film was conducted using an ozone-free xenon arc lamp with the excitation source of 305 nm with a pulse frequency of 50 kHz and power density of  $\sim 87 \times 10^{-6}$  W/m<sup>2</sup>. For the absorption measurement, the organic thin film was measured using a UV-visible spectrophotometer (Thermo Scientific Evolution 220). The measurement of time-resolved PL spectra was operated as following: the data were recorded by Spectra Pro 2300i monochromator system coupled with the ICCD detector, and the LS-2134 Nd:YAG laser system from LOTIS TII company was used as the pumping source. The prompt emission component acquired by an intensified charge coupled (ICCD) detector at zero delay time and a gate width of 100 ns is assigned to fluorescence, whereas the delayed components acquired at a delay time of 1 μs and gate

width 10  $\mu\text{s}$  is ascribed to the phosphorescence. The energy difference between the fluorescence and phosphorescence ( $\Delta E_{\text{ST}}$ ) were calculated from the emission onset of the prompt and delayed signals. PLQYs of thin films were determined using quantum yield spectrometer (Hamamatsu C9920-02). During the PLQY measurements, the integrating sphere was purged with pure and dry nitrogen to keep the environment inert. The selected monochromatic excitation light based on the absorption profile of blend films was used to excite samples placed in the integrating sphere. By comparing the spectral intensities of the monochromatic excitation light and the PL emission, the PLQY were determined. PLQY and absorption measurements were taken in an ambient environment. The experimental values of HOMO levels in solid state were determined with a Riken AC-2 photoemission spectrometer (PES).

The electrochemical properties were measured by cyclic voltammetry (CHI619B potentiostat). A glassy carbon electrode was used as a working electrode, and a platinum wire was used as a counter electrode. The oxidation potentials were conducted in dried dichloromethane (1.0 mM) with 0.1 M tetrabutylammonium hexafluorophosphate ( ${}^n\text{BuNPF}_6$ ) as the supporting electrolyte. The reduction potentials were conducted in dried tetrahydrofuran (for 1.0 mM) with 0.1 M tetrabutylammonium perchlorate ( ${}^n\text{BuNClO}_4$ ) as the supporting electrolyte and degassed by argon prior to the experiment. All the potentials were recorded versus Ag/AgCl as a reference electrode, further calibrated with the ferrocene/ferrocenium ( $\text{Fc}/\text{Fc}^+$ ) redox couple (0.48 eV in dichloromethane/ ${}^n\text{BuNPF}_6$  and 0.633 eV in tetrahydrofuran/ ${}^n\text{BuNClO}_4$ ). All the mass spectra were recorded by the National Taiwan University Mass Spectrometry-based Proteomics Core Facility by Bruker Daltonics Autoflex speed in MALDI-TOF mode.

### **Time-of-flight (TOF) mobility measurements**

Carrier-transport properties were studied by the time-of-flight (TOF) transient photocurrent technique in the structure: ITO glass/ **Tr-Ph** (1.1  $\mu\text{m}$ ) or **Tr-Tol** (0.97  $\mu\text{m}$ ) /Ag (200 nm), which were then placed inside a cryostat and kept under vacuum. The thickness of organic film was monitored in situ with a quartz sensor and calibrated by a thin film thickness measurement. A pulsed nitrogen laser (337 nm) was used as the excitation light source through the transparent electrode (ITO) inducing photogeneration of a thin sheet of excess carriers. Under an applied dc bias, the transient photocurrent was swept across the bulk of the organic film toward the collection

electrode (Ag), and then recorded with a digital storage oscilloscope. Depending on the polarity of the applied bias, selected carriers (holes or electrons) are swept across the sample with a transit time of  $t_T$ . With the applied bias  $V$  and the sample thickness  $D$ , the applied electric field  $E = V/D$ , and the carrier mobility is then given by  $\mu = D/(t_T E) = D^2/(V t_T)$ , in which the carrier transit time,  $t_T$ , can be extracted from the intersection of two asymptotes to the tail and plateau sections in the double logarithmic plots.

### **Device fabrication**

All chemicals were purified through vacuum sublimation prior to use. The OLEDs were fabricated through vacuum deposition of the materials at  $10^{-6}$  Torr onto the ITO-coated glass substrates having a sheet resistance of  $15 \Omega \text{ sq}^{-1}$ . Prior to use the ITO surface was cleaned ultrasonically; i.e. with acetone, methanol, and deionized water in sequence and finally with UV-ozone. The deposition rate of each organic material was ca.  $1\text{--}2 \text{ \AA s}^{-1}$ . The J–V–L characteristics of the devices were measured simultaneously in a glove-box. A programmable source measurement unit (2614B, Keithley) was used as a driving source of the device while the light intensity was measured by a calibrated silicon detector according to standard procedures.<sup>[8]</sup> The luminance was confirmed with a spectroradiometer (TOPCON BM-9A) in the visible region. EL spectra were measured using a photodiode array (Ocean Optics USB2000+). Accuracy after the consideration of both the variation in the device area and the instrumental accuracy was estimated to be around  $\pm 5\%$ .

### Synthesis of 5,10,15-tri-p-tolyl-10,15-dihydro-5H-diindolo[3,2-a:3',2'-c]carbazole

#### (Tr-Tol):

10,15-Dihydro-5H-diindolo[3,2-a:3',2'-c]carbazole (1.72 g, 5 mmol), 4-iodotoluene (5.02 g, 23 mmol), Pd(OAc)<sub>2</sub> (440 mg, 2 mmol), <sup>t</sup>Bu<sub>3</sub>PHBF<sub>4</sub> (1.13 g, 4 mmol) and NaO<sup>t</sup>Bu (4.32 g, 45 mmol) were mixed in a 250 mL two-neck bottle, and then the whole system was evacuated and purged with argon gas. Toluene (150 mL) was then added, and the reaction mixture was heated to reflux for 3 hours and then cooled down to room temperature. The solvent was removed *in vacuo*, dissolved in dichloromethane and filtrated to separate salt. The filtrate was then concentrated, and the crude product was purified by column chromatography on silica gel using the eluent system hexane:dichloromethane = 1 : 2 to give the product as pale-white solid. The obtained solid was then further purified by recrystallization by dichloromethane and hexane to obtain needle-like white solid. 5,10,15-tri-p-tolyl-10,15-dihydro-5H-diindolo[3,2-a:3',2'-c]carbazole (1.61 g, 50%). <sup>1</sup>H NMR (400 MHz, CD<sub>2</sub>Cl<sub>2</sub>) δ 7.54 (d, *J* = 8.4 Hz, 2H), 7.44 (d, *J* = 8.4 Hz, 2H), 7.31 (d, *J* = 8.4 Hz, 1H), 7.16 (t, *J* = 7.6 Hz, 1H), 6.78 (t, *J* = 8 Hz, 1H), 6.10 (d, *J* = 8.4 Hz, 1H), 2.57 (s, 3H) <sup>13</sup>C NMR (100 MHz, CDCl<sub>3</sub>) δ 141.64, 138.17, 137.81, 130.41, 128.81, 122.64, 122.40, 119.62, 109.81, 104.04, 21.36. HRMS (*m/z*, MALDI) calcd for C<sub>45</sub>H<sub>33</sub>N<sub>3</sub> 615.2669 found 615.2689; Elemental anal. calcd for C<sub>45</sub>H<sub>33</sub>N<sub>3</sub>:C, 87.77; H, 5.40; N, 6.82 found C, 87.86; H, 5.27; N, 6.79.

### Synthesis of 2,4,6-tris(3-(1H-pyrazol-1-yl)phenyl)pyrimidine(3P-T2P):

2,4,6-tris(3-bromophenyl)pyrimidine (1.09 g, 2 mmol), 1H-pyrazole (0.82 g, 12 mmol), CuI (108 mg, 1.2 mmol), Cs<sub>2</sub>CO<sub>3</sub> (3.91 g, 12 mmol) were mixed in a 100 mL two-neck bottle, and then the whole system was evacuated and purged with argon gas. Degassed DMF (20 mL) was then added *via* syringe, and the reaction mixture was heated to reflux for 4 days and then cooled down to room temperature. The reaction mixture was poured into water to form precipitate, filtered to separate from solvent, and the solid was then dissolved in dichloromethane and pass through a plug of Celite to remove salt. The filtrate was extracted with brine, and the organic layer was dried over magnesium sulfate. The solvent was then concentrated, and the crude product was purified by column chromatography on silica gel using chloroform as eluent to give the product as white solid of 2,4,6-tris(3-(1H-pyrazol-1-yl)phenyl)pyrimidine (400 mg

0.79mmol, 39.5%)  $^1\text{H}$  NMR (400 MHz,  $\text{CD}_2\text{Cl}_2$ )  $\delta$  9.06 – 8.92 (m, 1H), 8.65 (ddd,  $J$  = 7.8, 3.3, 1.5 Hz, 3H), 8.32 – 8.22 (m, 2H), 8.19 (s, 1H), 8.15 (dd,  $J$  = 5.0, 2.4 Hz, 3H), 7.97 – 7.85 (m, 3H), 7.78 (dd,  $J$  = 3.8, 1.7 Hz, 3H), 7.71 – 7.58 (m, 3H), 6.62 – 6.48 (m, 3H).  $^{13}\text{C}$  NMR (100 MHz,  $\text{CD}_2\text{Cl}_2$ )  $\delta$  164.81, 164.29, 141.82, 141.62, 141.46, 141.22, 139.83, 139.15, 130.60, 130.19, 127.52, 127.50, 126.87, 125.71, 121.99, 121.83, 119.29, 118.34, 111.80, 108.43, 108.17. HRMS ( $m/z$ , MALDI) calcd for  $\text{C}_{31}\text{H}_{23}\text{N}_8$  506.1967 found 507.2058 ( $M+1$ ); Elemental anal. calcd for  $\text{C}_{31}\text{H}_{23}\text{N}_8$ :C, 73.50; H, 4.38; N, 22.12 found C, 73.47; H, 4.35; N, 22.12.

Synthesis of 2,4,6-tris(3-(1H-pyrazol-1-yl)phenyl)pyridine (**3P-Pyr**):

2,4,6-tris(3-bromophenyl)pyridine (5.45 g, 10 mmol), 1H-pyrazole (4.09 g, 60 mmol), CuI (543 mg, 6 mmol),  $\text{Cs}_2\text{CO}_3$  (20.0 g, 60 mmol) were mixed in a 100 mL two-neck bottle, and then the whole system was evacuated and purged with argon gas. Degassed DMF (20 mL) was then added *via* syringe, and the reaction mixture was heated to reflux for 4 days and then cooled down to room temperature. The reaction mixture was poured into water to form precipitate, filtered to separate from solvent, and the solid was then dissolved in dichloromethane and pass through a plug of Celite to remove salt. The filtrate was extracted with brine, and the organic layer was dried over magnesium sulfate. The solvent was then concentrated, and the crude product was purified by column chromatography on silica gel using chloroform as eluent to give the product as white solid of 2,4,6-tris(3-(1H-pyrazol-1-yl)phenyl)pyridine (1.8 g, 3.56 mmol, 36%)  $^1\text{H}$  NMR (400 MHz,  $\text{CD}_2\text{Cl}_2$ )  $\delta$  8.61 (t,  $J$  = 1.9 Hz, 2H), 8.23 – 8.16 (m, 3H), 8.14 (dd,  $J$  = 2.5, 0.5 Hz, 2H), 8.12 – 8.07 (m, 3H), 7.83 (ddt,  $J$  = 8.0, 2.5, 1.3 Hz, 3H), 7.78 – 7.70 (m, 4H), 7.65 (td,  $J$  = 7.9, 4.4 Hz, 3H), 6.56 – 6.51 (m, 3H).  $^{13}\text{C}$  NMR (100 MHz,  $\text{CD}_2\text{Cl}_2$ )  $\delta$  157.25, 150.46, 141.84, 141.63, 141.55, 141.38, 141.23, 140.75, 130.80, 130.39, 127.50, 125.76, 125.55, 120.30, 120.01, 118.50, 118.40, 118.26, 108.45, 108.21. HRMS ( $m/z$ , MALDI) calcd for  $\text{C}_{32}\text{H}_{24}\text{N}_7$  505.2015 found 506.2106 ( $M+1$ ); Elemental anal. calcd for  $\text{C}_{32}\text{H}_{24}\text{N}_7$ :C, 76.02; H, 4.59; N, 19.39 found C, 75.92; H, 4.64; N, 19.31.

Synthesis of 1,3-bis(4-(di-*p*-tolylamino)phenyl)benzo[*c*]thiophene-5,6-dicarbonitrile ((**DT**)<sub>2</sub>**BTh2CN**):

The mixture of compound 1,3-dibromobenzo[*c*]thiophene-5,6-dicarbonitrile (0.68 g,

2.00 mmol), [4-[bis(4-methylphenyl)amino] phenyl]boronic acid (1.52 g, 4.80 mmol), Pd(PPh<sub>3</sub>)<sub>4</sub> (0.23 g, 0.20 mmol), and K<sub>2</sub>CO<sub>3</sub> (1.1 g, 8.00 mmol) were dissolved in toluene (20.0 mL) and deionized water (4.0 mL) and refluxed under argon for 24 h. After the removal of toluene, the product was extracted with dichloromethane and water, dried over MgSO<sub>4</sub> and concentrated to give a crude product, which was then purified by column chromatography with the eluent of dichloromethane / hexane = 1 / 1 to afford orange solid as product of 1,3-bis(4-(di-p-tolylamino)phenyl)benzo[c]thiophene-5,6-dicarbonitrile (1.16 g, 80 %). <sup>1</sup>H NMR (400 MHz, CD<sub>2</sub>Cl<sub>2</sub>) δ 8.30 (s, 2H), 7.43 (d, *J* = 8.4 Hz, 4H), 7.20–7.04 (m, 20H), 2.35 (s, 12H) ; <sup>13</sup>C NMR (100 MHz, CD<sub>2</sub>Cl<sub>2</sub>) δ 149.8, 145.0, 140.7, 134.5, 132.3, 132.0, 130.9, 130.7, 130.6, 130.4, 126.0, 124.4, 121.9, 117.5, 106.9, 21.2 HRMS (*m/z* , MALDI) calcd for C<sub>50</sub>H<sub>38</sub>N<sub>4</sub>S 726.2817 found 726.2900.

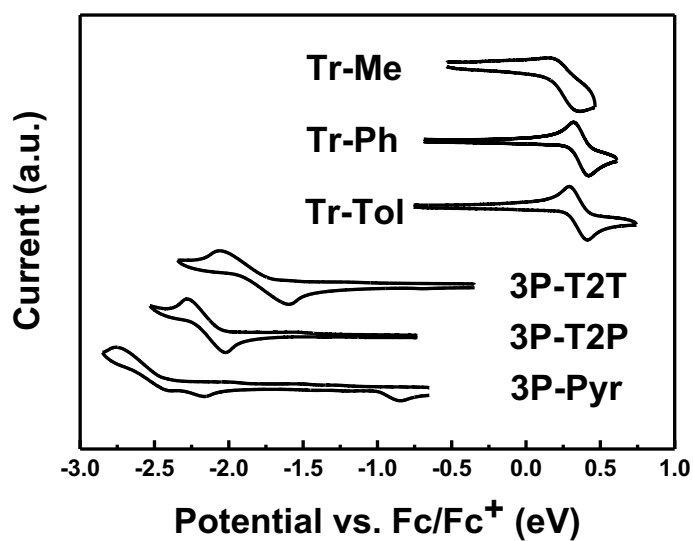


**Figure S1.** Cyclic voltammograms of triazatruxenes **Tr-Me**, **Tr-Ph**, **Tr-Tol**, and acceptors **3P-T2T**, **3P-T2P** and **3P-Pyr**.

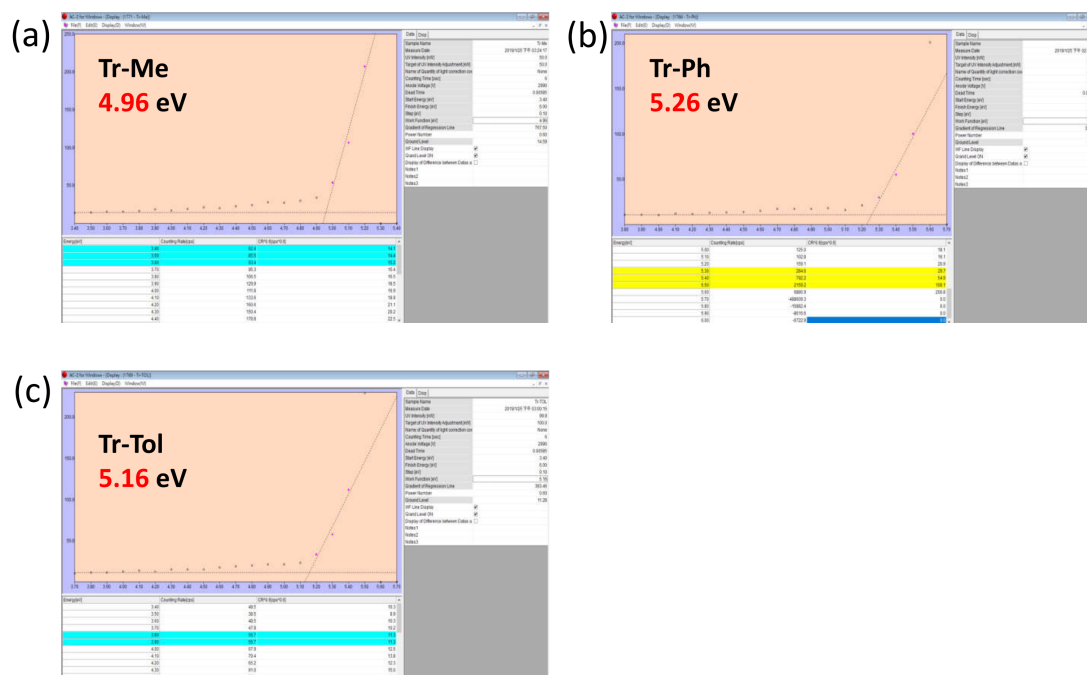


**Figure S2.** HOMO energy levels of (a) **Tr-Me**, (b) **Tr-Ph** and (c) **Tr-Tol** determined by using photoelectron yield spectroscopy (Riken AC-2).

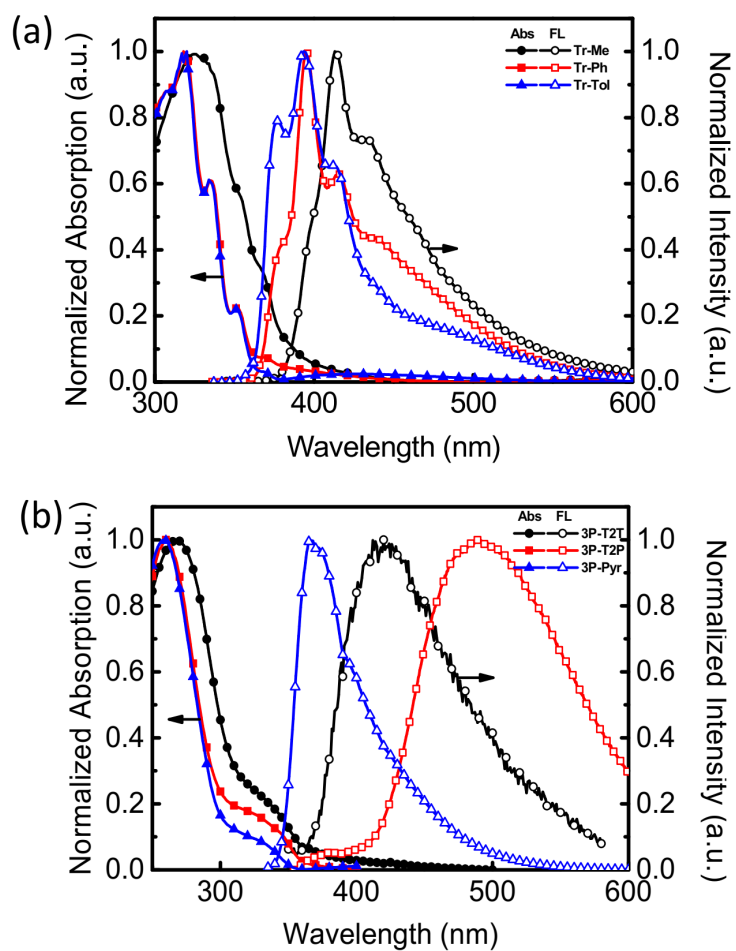


**Figure S3.** UV-Vis and emission spectra of (a) donors (**Tr-Me**, **Tr-Ph** and **Tr-Tol**) and (b) acceptors (**3P-T2T**, **3P-T2P** and **3P-Pyr**) in neat film recorded at room temperature.

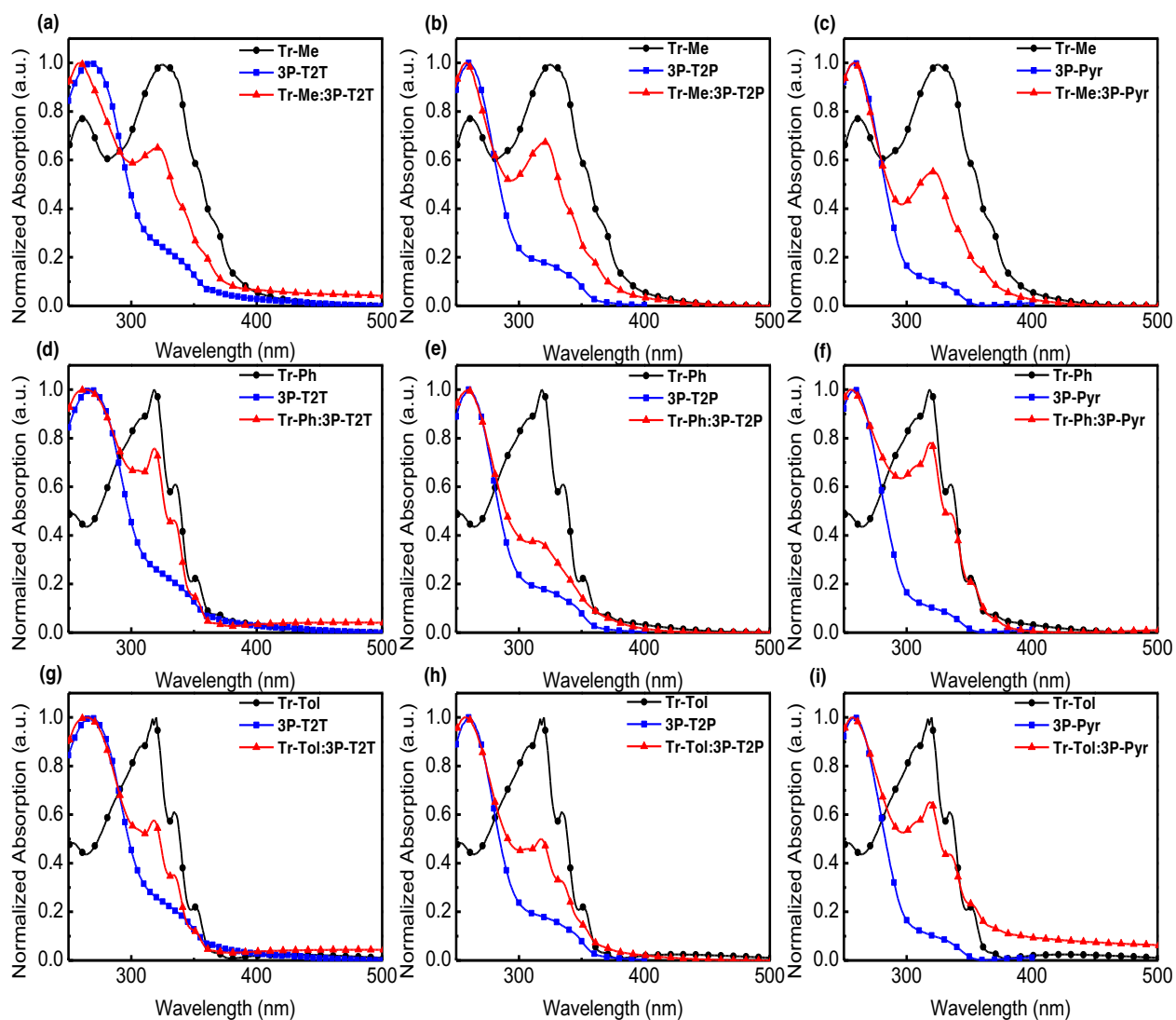


**Figure S4.** UV-Vis of D-A blend film and their corresponding composing materials recorded in room temperature.

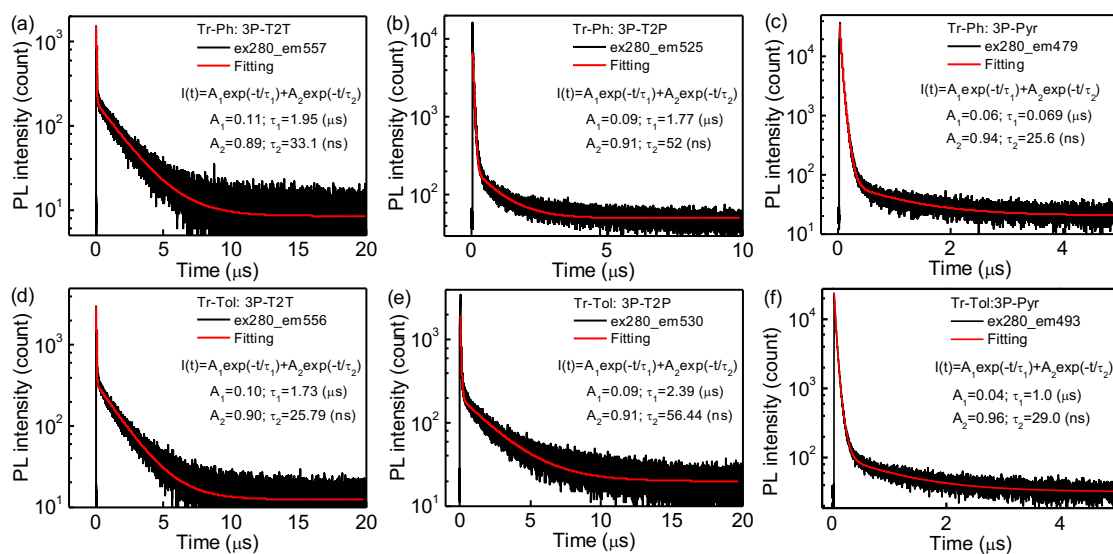


**Figure S5.** Transient PL decays of donor: acceptor (1:1) film at room temperature.

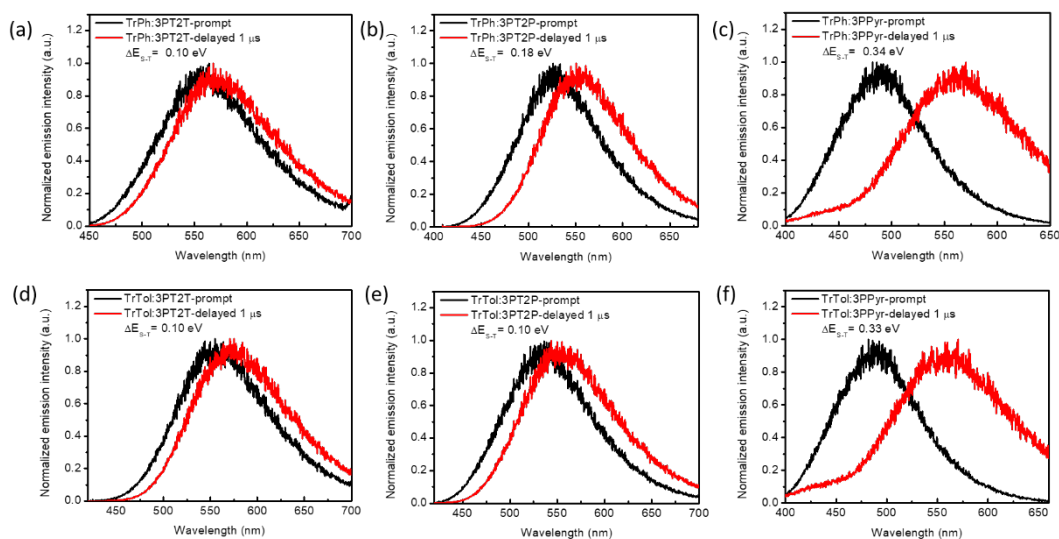


**Figure S6.** Time-resolved PL spectra of the donor: acceptor (1:1) films at 300 K. Prompt (black line: delay = 0 ns, gate width 100 ns) and delayed 1  $\mu$ s (red line: gate width = 10  $\mu$ s) components of the PL spectra.  $\Delta E_{ST}$  is calculated from the energy difference between the emission onsets of prompt and delayed signals.

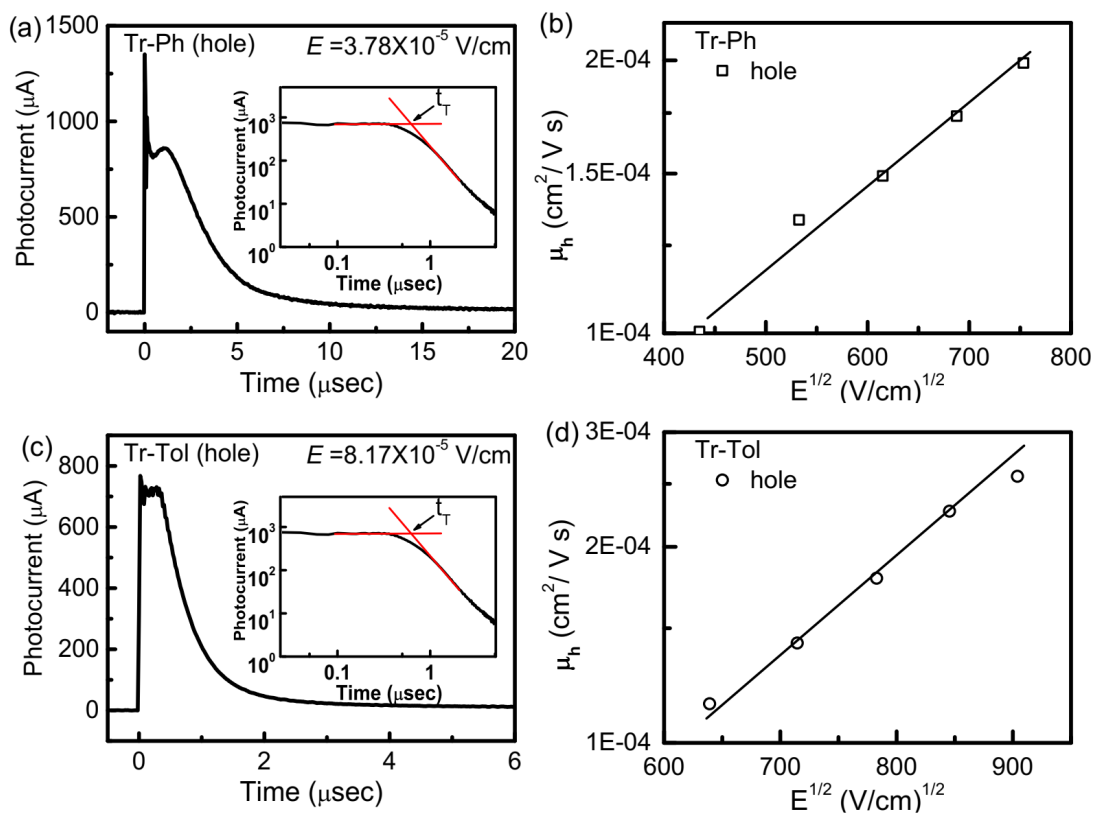


**Figure S7.** Typical transient photocurrent signals for hole (a) **Tr-Ph** ( $E = 3.78 \times 10^5 \text{ V/cm}$ ) and (c) **Tr-Tol** ( $E = 8.17 \times 10^5 \text{ V/cm}$ ). Insets are the double logarithmic plots of (a)/(c). Electron and hole mobilities versus  $E^{1/2}$  for (b) **Tr-Ph** and (d) **Tr-Tol**.

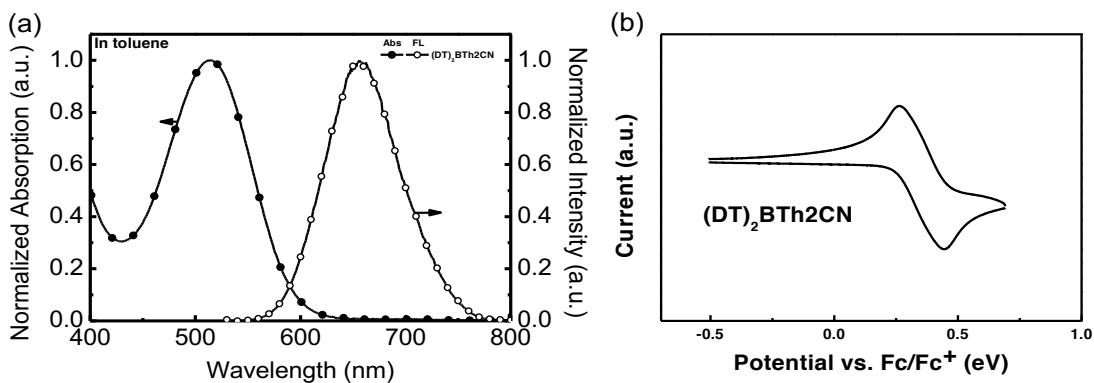


**Figure S8.** (a) UV-Vis and emission spectra and (b) cyclic voltammogram of  $(DT)_2BTh2CN$ .

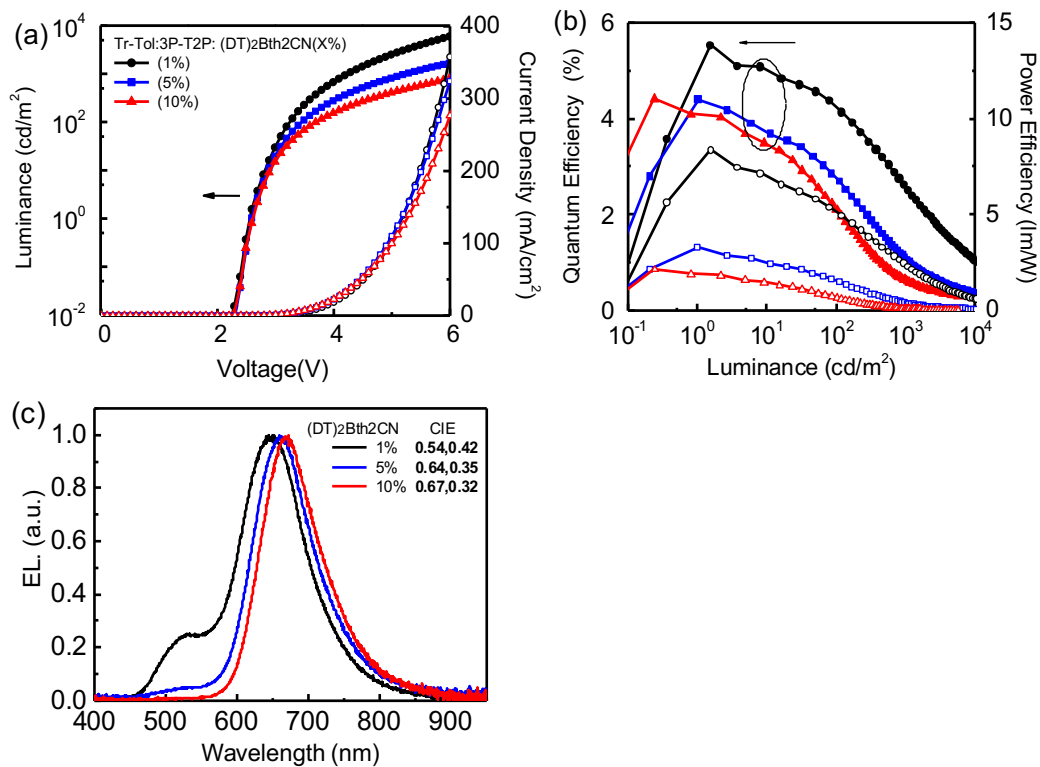


**Figure S9.** (a) J–V–L characteristics, (b) EQE and PE as a function of luminance and (c) EL spectra of **Tr-Tol:3P-T2P** hosted devices with various doping concentrations.

**Table S1.** Characterization of **(DT)<sub>2</sub>BTh2CN**.

Molecule	$\lambda_{\max}$ <sup>a</sup> (nm)	PL $\lambda_{\max}$ (nm) <sup>a</sup>	PL <sub>onset</sub> nm (eV) <sup>a</sup>	E <sub>g</sub> (eV) <sup>b</sup>	HOMO (eV) <sup>c</sup>	LUMO (eV) <sup>d</sup>	T <sub>d</sub> (°C)
<b>(DT)<sub>2</sub>BTh2CN</b>	515	660	371	2.09	-5.17 <sup>b</sup>	-3.08 <sup>c</sup>	408

<sup>a</sup> Data observed in toluene.

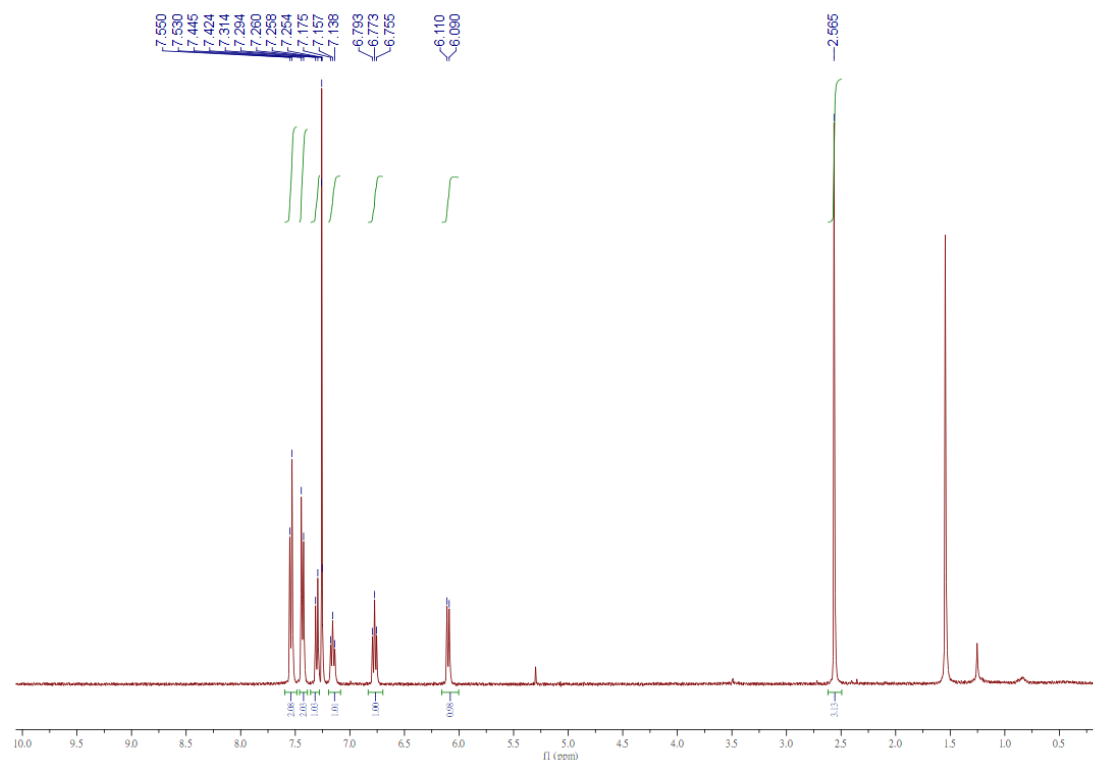
<sup>b</sup> Estimated from the onset of UV-Vis absorption spectra.

<sup>c</sup> Calculated from potential vs. ferrocene/ferrocenium redox couple.

<sup>d</sup> Calculated by the difference from HOMO/LUMO and corresponding optical bandgap.

**Table S2.** The PLQY and TRPL characteristics of the 10 wt% **(DT)<sub>2</sub>Bth2CN** doped in D:A blended films.

Donor	Acceptor	PLQY		TRPL analysis		
		(%)	A <sub>1</sub>	$\tau_p$ (ns)	A <sub>2</sub>	$\tau_d$ ( $\mu$ s)
<b>Tr-Ph</b>	<b>3P-T2T</b>	40	0.99	6.89	0.01	0.15
	<b>3P-T2P</b>	50	0.98	7.80	0.02	0.12
<b>Tr-Tol</b>	<b>3P-T2T</b>	37	0.99	6.60	0.003	0.10
	<b>3P-T2P</b>	47	0.99	7.80	0.002	0.12

**Figure S10.** The <sup>1</sup>H NMR of **Tr-Tol**.

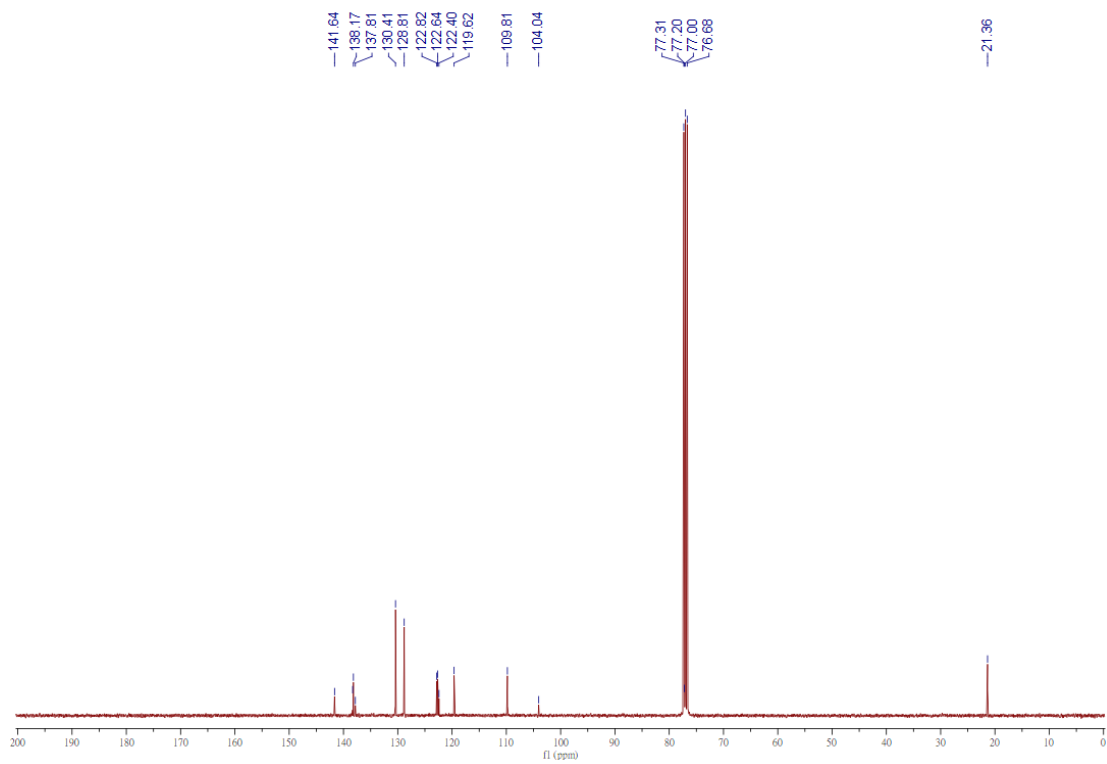


**Figure S11.** The  $^{13}\text{C}$  NMR of Tr-Tol.

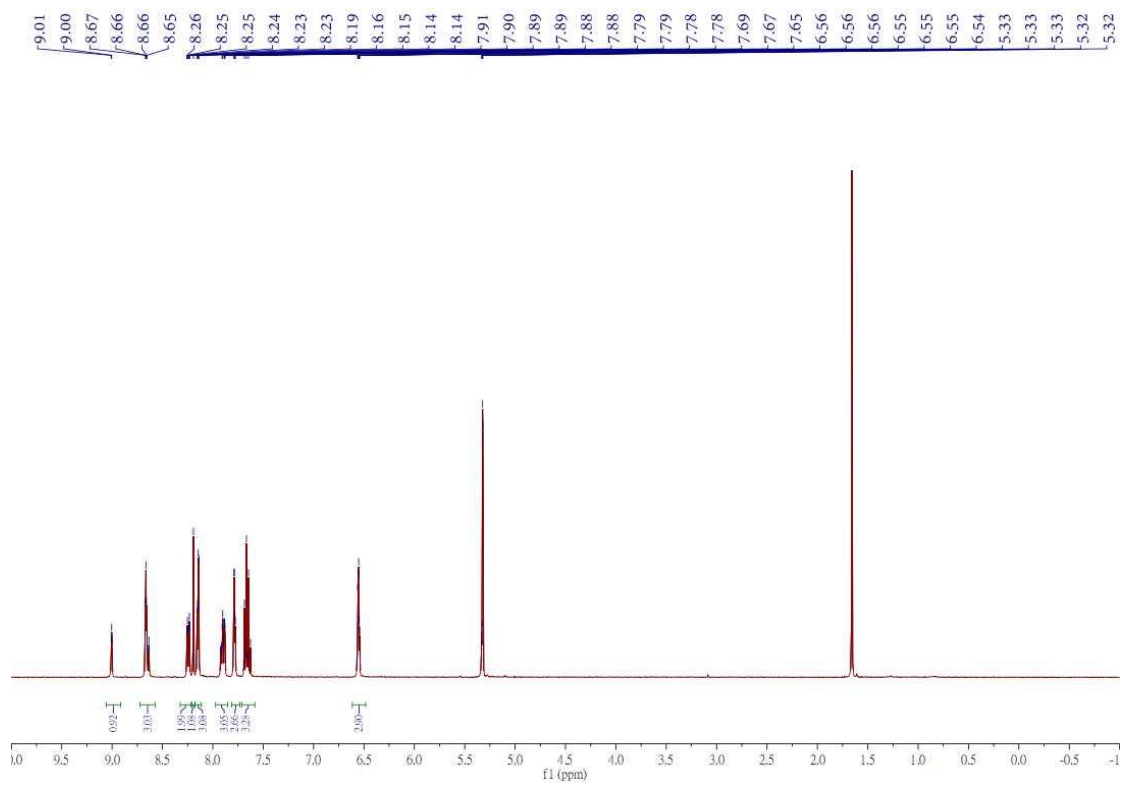


**Figure S12.** The  $^1\text{H}$  NMR of 3P-T2P.

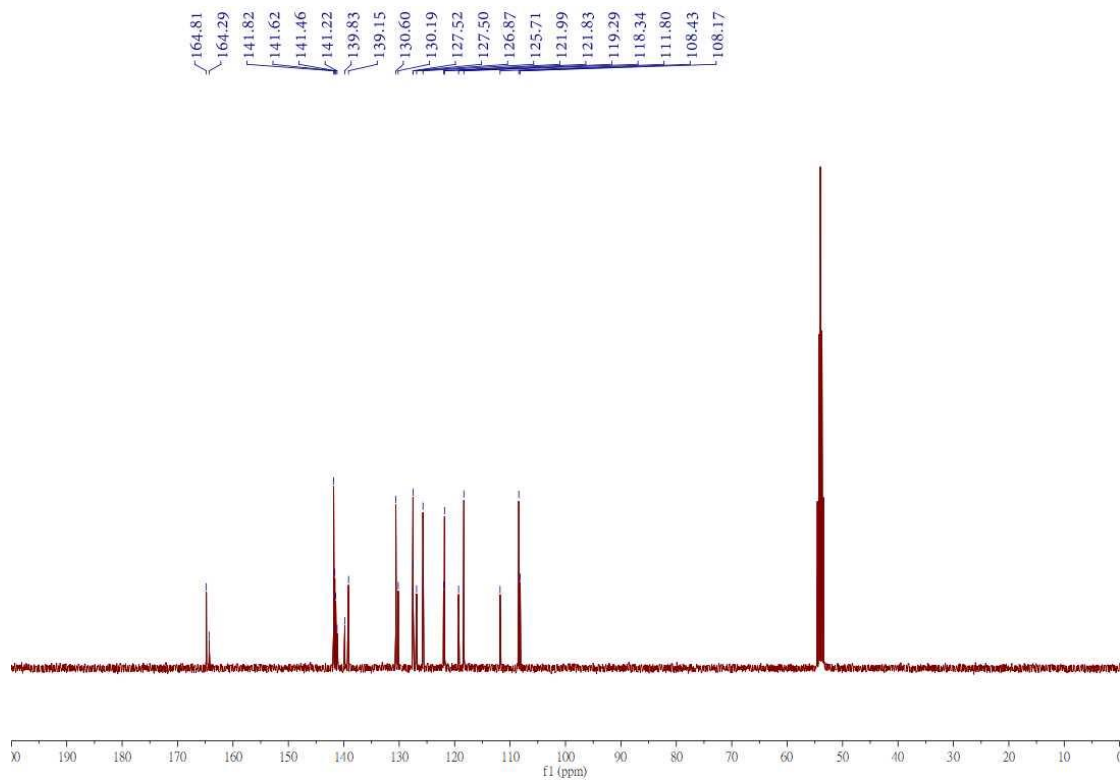


**Figure S2.** The  $^{13}\text{C}$  NMR of 3P-T2P.

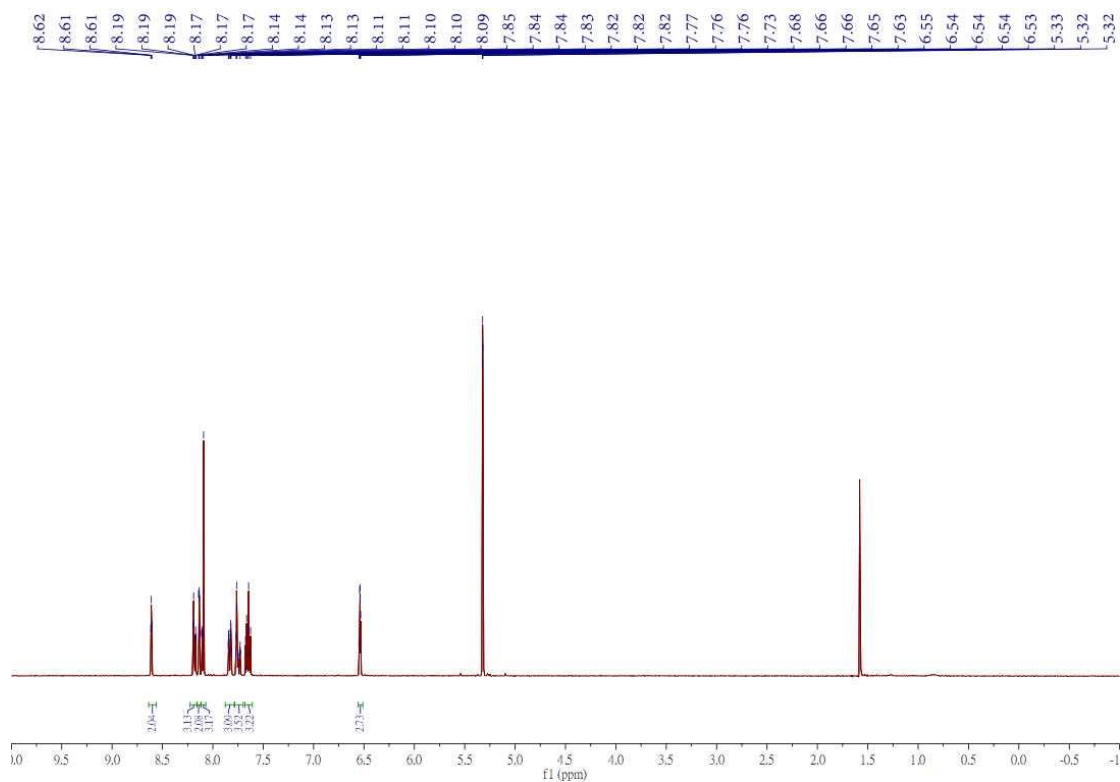


**Figure S3.** The  $^1\text{H}$  NMR of 3P-Pyr.

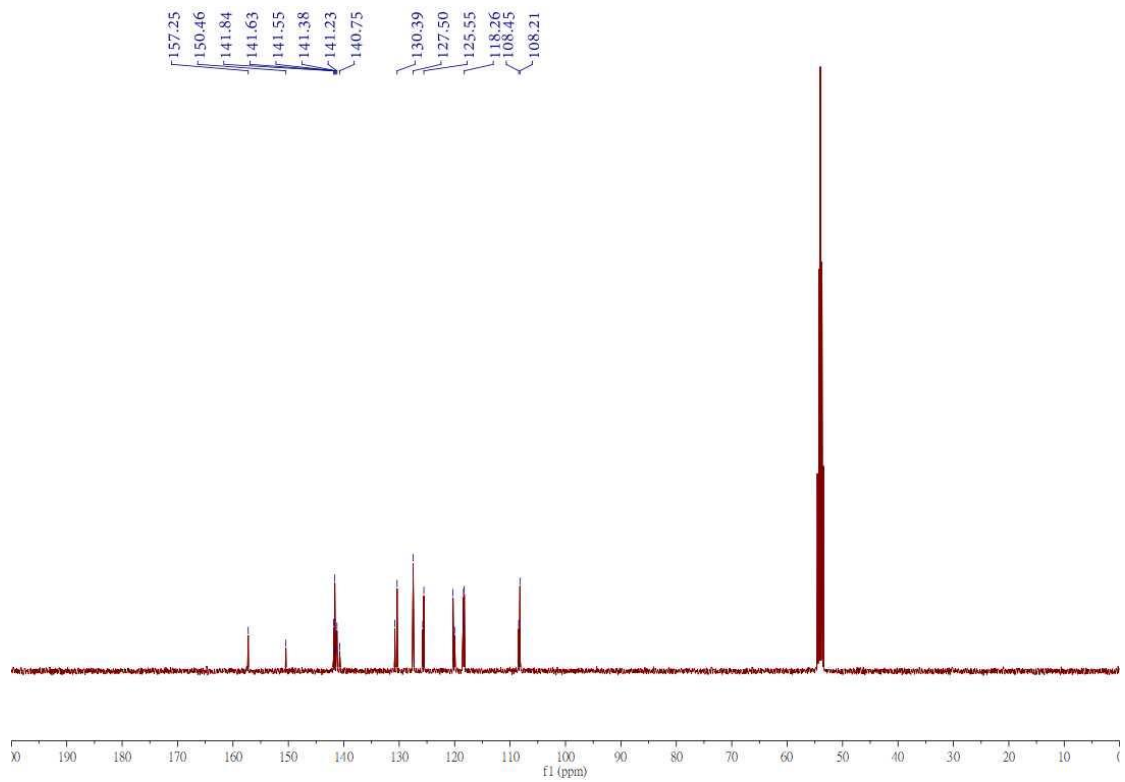


**Figure S4.** The  $^{13}\text{C}$  NMR of 3P-Pyr.

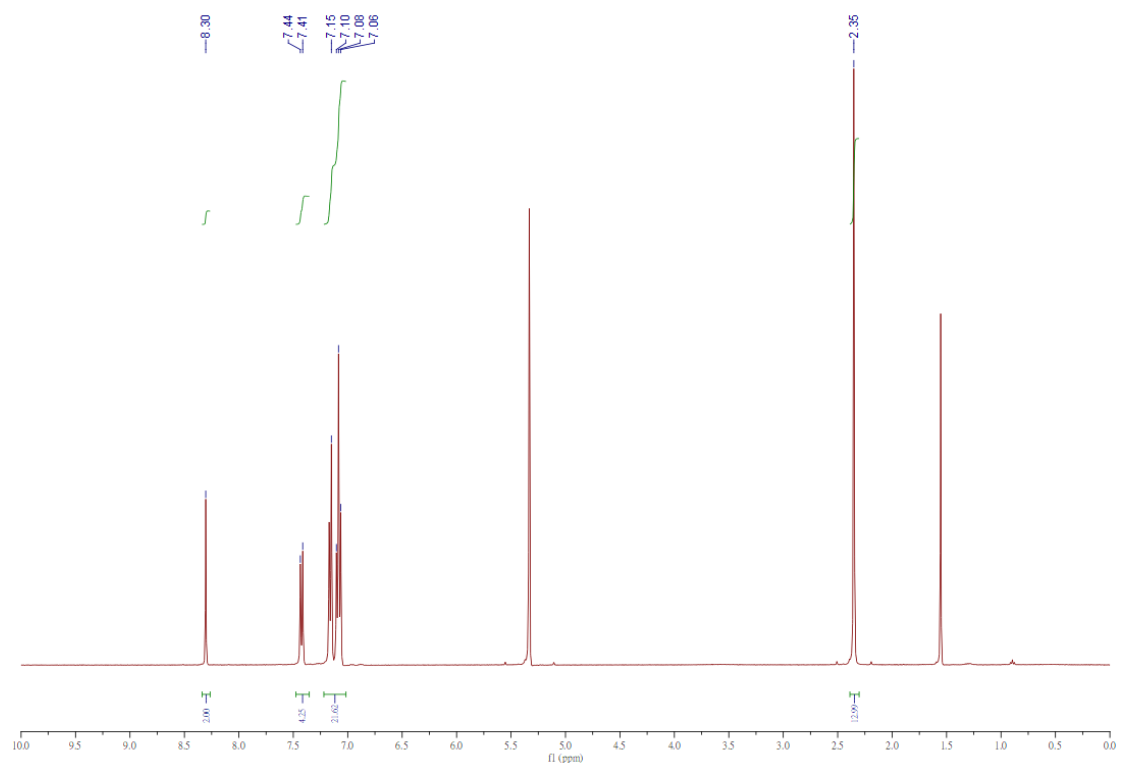


**Figure S16.** The  $^1\text{H}$  NMR of  $(\text{DT})_2\text{BTh}_2\text{CN}$ .

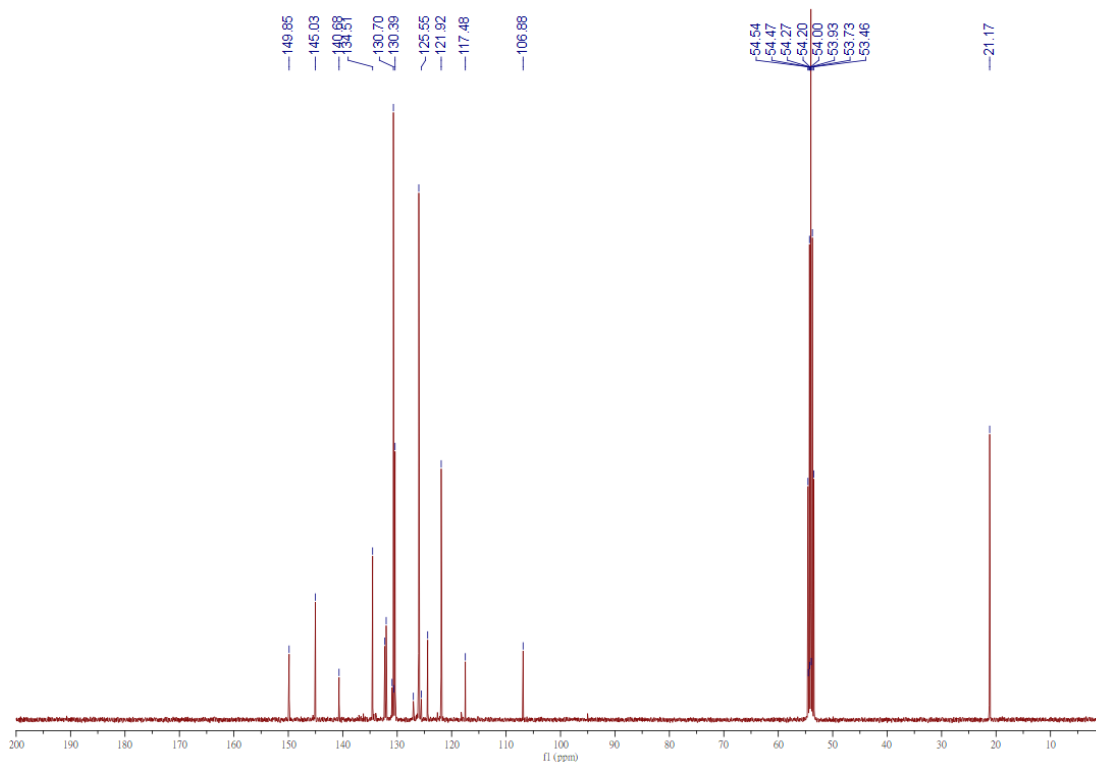


**Figure S17.** The  $^{13}\text{C}$  NMR of  $(\text{DT})_2\text{BTh}2\text{CN}$ .

### Reference

1. M. Franceschin, L. G.-Satriani, A. Alvino, G. Ortaggi and A. Bianco, Study of a convenient method for the preparation of hydrosoluble fluorescent triazatruxene derivatives. *Eur. J. Org. Chem.*, **2010**, 134–141.
2. J. D. Douglas, G. Griffini, T. W. Holcombe, E. P. Young, O. P. Lee, M. S. Chen and J. M. J. Fréchet, Functionalized isothianaphthene monomers that promote quinoidal character in donor–acceptor copolymers for organic photovoltaics. *Macromolecules*, 2012, **45**, 4069–4074.
3. S.-J. Su, C. Cai and J. Kido, Three-carbazole-armed host materials with various cores for RGB phosphorescent organic light-emitting diodes. *J. Mater. Chem.*, 2012, **22**, 3447-3456.
4. A. G. Martinez, A. H. Fernandez, F. M. Jimenez, A. G. Fraile, L. R. Subramanian and M. Hanack, On the mechanism of the reaction between ketones and trifluoromethanesulfonic anhydride. An improved and convenient method for the preparation of pyrimidines and condensed pyrimidines. *J. Org. Chem.*, 1992, **57**, 1627-1630.

5. D. H. Huh, G. W. Kim, G. H. Kim, C. Kulshreshtha and J. H. Kwon, High hole mobility hole transport material for organic light-emitting devices. *Synth. Met.*, 2013, **180**, 79–84.
6. Gyeong Woo Kim, Raju Lampande, Dong Cheol Choe, Hyeong Woo Bae, Jang Hyuk Kwon, Efficient hole injection material for low operating voltage blue fluorescent organic light emitting diodes. *Thin Solid Films*, 2015, **589**, 105–110.
7. H.-F. Chen, T.-C. Wang, S.-W. Lin, W.-Y. Hung, H.-C. Dai, H.-C. Chiu, K.-T. Wong, M.-H. Ho, T.-Y. Cho, C.-W. Chen and C.-C. Lee, Peripheral modification of 1,3,5-triazine based electron-transporting host materials for sky blue, green, yellow, red, and white electrophosphorescent devices. *J. Mater. Chem.*, **2012**, 22, 15620-15627.
8. S. R. Forrest, D. C. Bradley and M. E. Thompson, Measuring the Efficiency of Organic Light-Emitting Devices. *Adv. Mater.*, **2003**, 15, 1043–1048.